Electronic Supplementary Material (ESI) for Journal of Materials Chemistry A.

Hierarchical confine of PtZn alloy nanoparticles and single-dispersed Zn atoms on COF@MOF-derived carbon towards efficient oxygen reduction reaction

Yu Guo, †[a] Shuai Yang, †[bc] Qing Xu,[ac]* Ping Wu,[ac] Zheng Jiang,[bc] and Gaofeng Zeng [ac]*

Experimental Section

***Materials*:** 2-Methylimidazole (purity for all chemicals) and platinum nitrate solution (18.02 wt.% Pt) were purchased from Aladdin. 2,4,6-Trihydroxyben-zene-1,3,5-tricarbaldehyde (TP) and [2,2'-bipyridine]-5,5'-diamine (BPY) were purchased from Alfa. Zinc nitrate hexahydrate, methanol (MeOH), tetrahydrofuran (THF), ethanol (EtOH), potassium hydroxide (KOH) and perchloric acid ($HClO_4$) were from Sinopharm Chemical Reagent Co.,Ltd.

Catalyst preparation: ZIF-8 nanocrystals were synthesized from 2-methylimidazole and zinc nitrate hexahydrate (recipe contents) by solvothermal method (reaction conditions e.g. solvent temp. time). [16]

In the synthesis of COF@MOF, 257.32 mg of TP in 30 mL THF and 345.56 mg of BPY in 30 mL THF were added into the mixture of ZIF-8 (600 mg) and THF (340 mL), which were then sonicated for 30 mins and stirred at 25 °C for 24 h to obtain ZIF-8 supported TP-BPY-COF. The solid was washed with MeOH and THF in sequence and then dried in vacuum to yield COF@MOF with an isolation TP-BPY-COF yield of 81%. For the synthesis of Pt-COF@MOF, 1.0 g COF@MOF was well-dispersed in 500 mL EtOH, followed by adding 200 µL $Pt(NO_3)_2$ solution and stirring for 24 h at room temperature. The products were washed with EtOH and THF and then dried in vacuum to obtain 750 mg Pt-COF@MOF. The as-prepared Pt-COF@MOF was heated at 800 °C for 1 h (5 °C min^{-1}) in N_2 to yield Pt-COF@MOF_{800}.

ORR performance tests: The catalyst (5 mg) was ultrasonic dispersed in a Nafion ethanol solution (0.25wt%, 500 μL) for 2 h to yield a homogeneous ink. The catalyst ink (12 μL) was pipetted onto a glassy carbon electrode (d = 5.00 mm, S = 0.196 cm^2) with a loading amount of 0.6 mg cm^{-2}. The commercial Pt/C catalyst (20 wt% platinum on carbon black, BASF) was employed as a reference. The Pt/C catalyst ink and electrode were prepared by the same conditions to that of Pt-COF@MOF_{800}. All the electrochemical measurements were conducted in a conventional three-electrode cell using the PINE electrochemical workstation (Pine Research Instrumentation, USA) at room temperature. The Ag/AgCl (3 M KCl) and platinum wire were used as reference and counter electrodes, respectively. A rotating ring disk electrode (RRDE) electrode with a Pt ring and a glassy carbon disk served as the substrate for the working electrode for evaluating the ORR activity and selectivity of various catalysts. The electrochemical experiments were conducted in O_2 saturated aqueous solution of KOH (0.1 M) or $HClO_4$ (0.1 M) for ORR. The RRDE measurements were conducted at a rotation rate of 1600 rpm with a sweep rate of 10 mV s^{-1}. On the basis of ring and disk currents, the electron-transfer number (n) and four-electron selectivity of catalysts based on the H_2O_2 yield (H_2O_2 (%)) were calculated from the equations of $n = 4 I_D/[(I_R/N) + I_D]$ and H_2O_2 (%) $= 200 (I_R/N)/[(I_R/N) + I_D]$, where I_D and I_R are the disk and ring currents, respectively, and the ring collection efficiency N is 0.37. The Tafel slope was estimated by linear fitting of the polarization curves according to the Tafel equation ($\eta = b \times \log j + a$, where j is the current density and b is the Tafel slope). For the cyclic voltammetry (CV) tests, the potential range was circularly scanned between 0.15 and 1.1 V at a scan rate of 50 mV s^{-1} after purging O_2 gas for 30 min. To estimate the double layer capacitance, the electrolyte was deaerated by bubbling with nitrogen, and then the voltammogram was evaluated again in the deaerated electrolyte. The Nyquist plots were obtained at 0.7 V, from 100,000 to 0.1 HZ with a potential amplitude of 10 mV.

Characterizations: Powder X-ray diffraction (PXRD) data were recorded on an Ultima IV diffractometer with Cu Kα radiation by depositing powder on glass substrate, from 2ϑ = 1.5° up to 60° with 0.02° increment. Nitrogen sorption isotherms were measured at 77 K with a TriStar II, Micromeritics. The Brunauer-Emmett-Teller (BET) method was utilized to calculate the specific surface areas. By using the non-local density functional theory (NLDFT) model, the pore volume was derived from the sorption curve. X-ray photoelectron spectroscopy (XPS) measurements were carried out on a Thermo Scientific K-Alpha XPS spectrometer using Al Kα X-ray source for radiation. Raman spectra were obtained from a Bruker SEN TERRA spectrometer employing a semiconductor laser (λ = 532 nm). High-resolution

transmission electron microscope images were obtained by Transmission electron microscopy (TEM, FEI Tecnai G2) installed with energy dispersive spectrometer (EDS, Oxford).

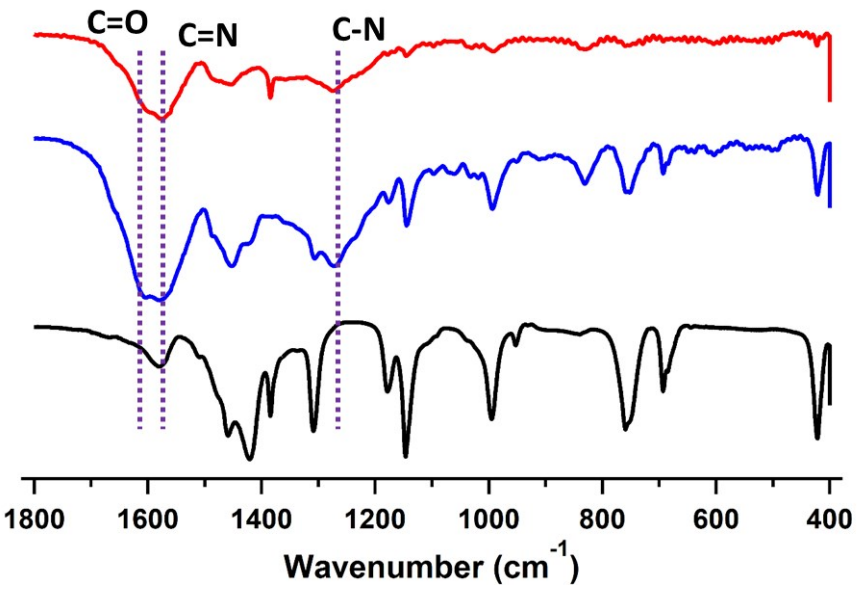

Figure S1. FT IR spectra of ZIF-8 (black), COF@MOF (blue) and Pt-COF@MOF (red).

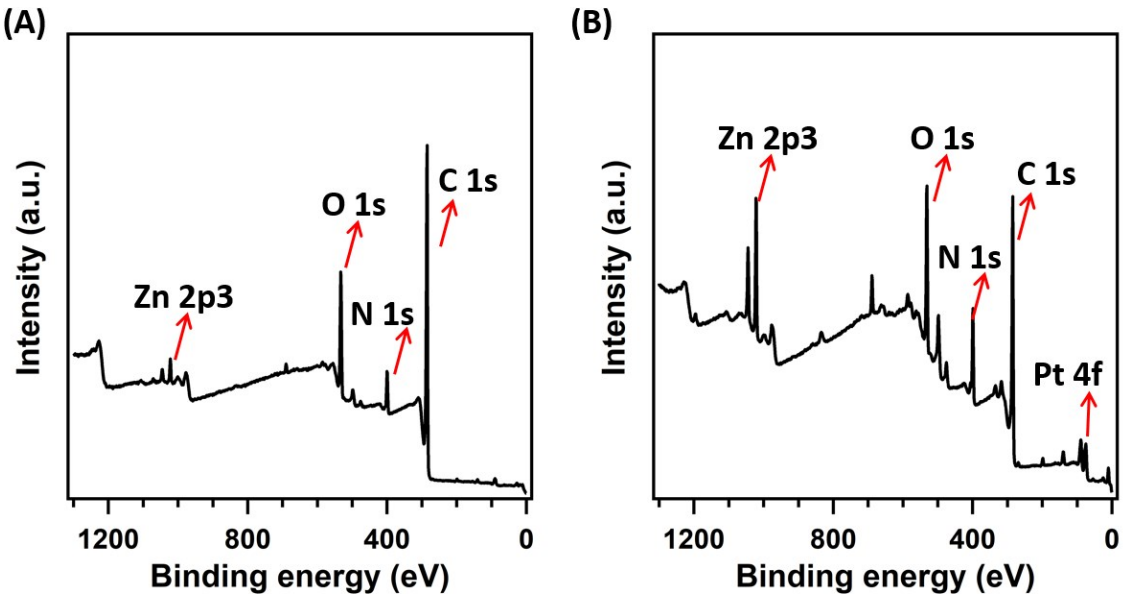

Figure S2. XPS spectra of COF@MOF and Pt-COF@MOF.

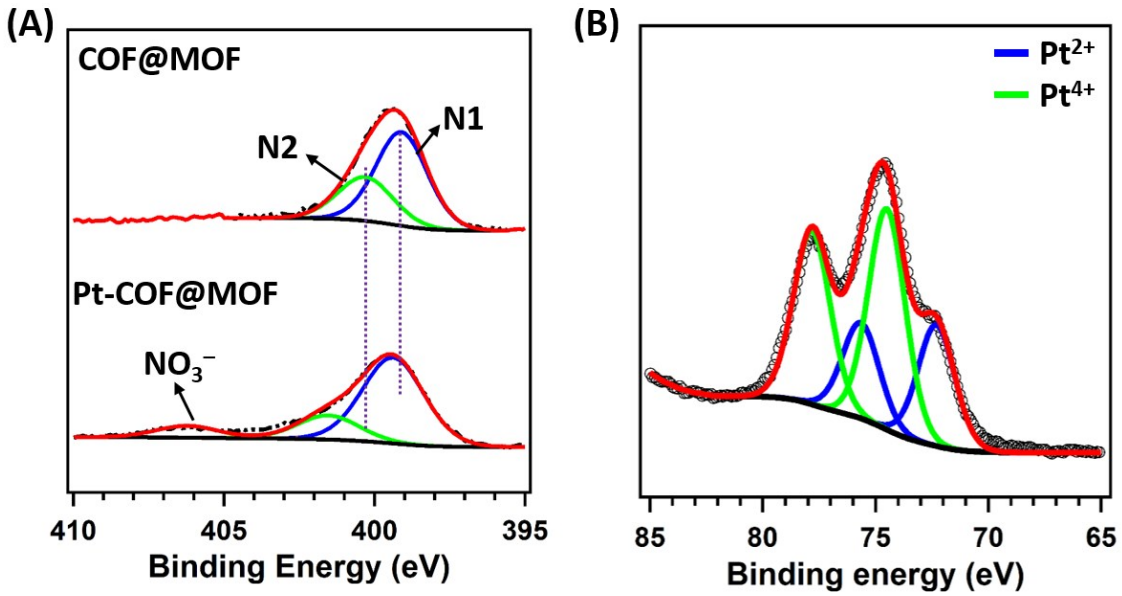

Figure S3. (A) High-resolution XPS spectra of N 1s for COF@MOF and Pt-COF@MOF. (B) High-resolution XPS spectra of Pt 4f for Pt-COF@MOF.

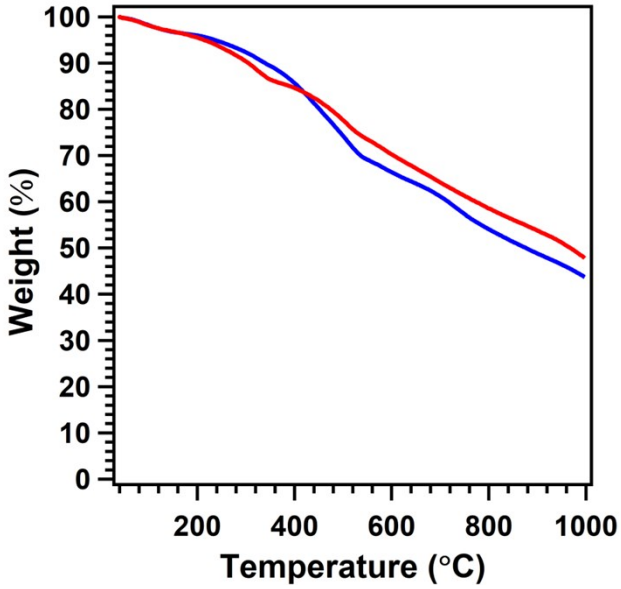

Figure S4. TGA profiles for COF@MOF (blue curves) and Pt-COF@MOF (red curve) from 25 to 1000 °C under N_2.

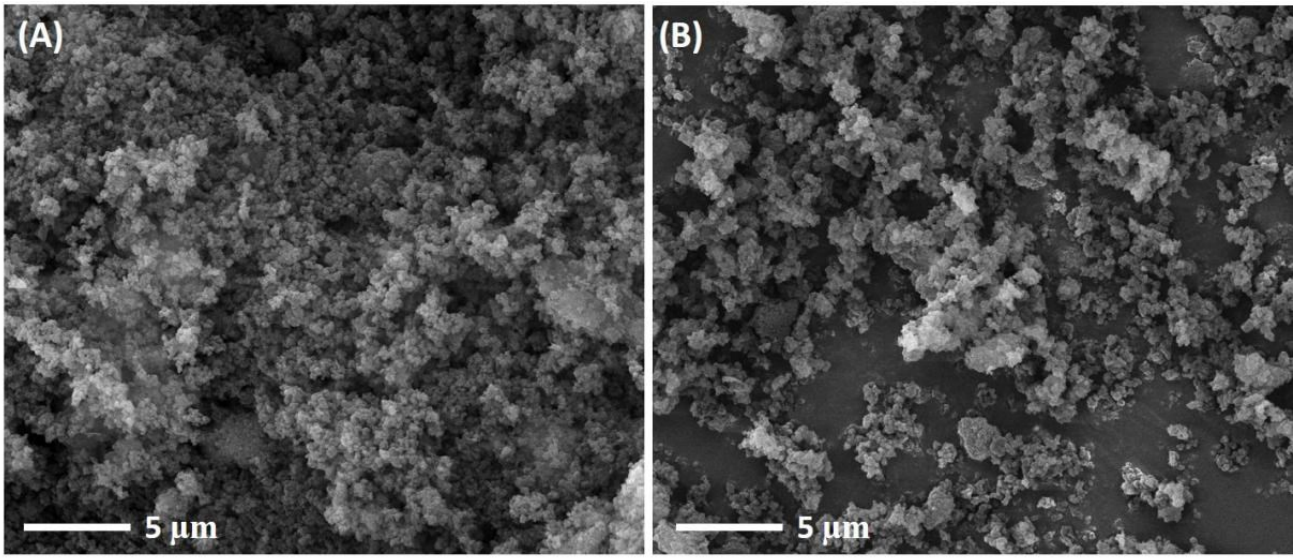

Figure S5. SEM images of (A) COF@MOF and (B) Pt-COF@MOF.

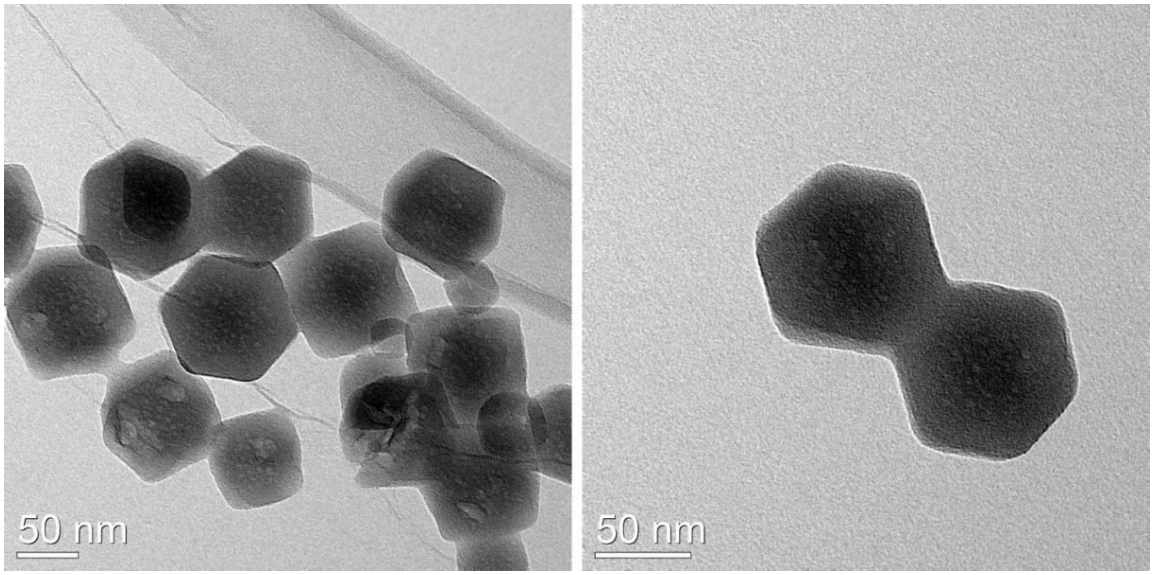

Figure S6. TEM images of ZIF-8.

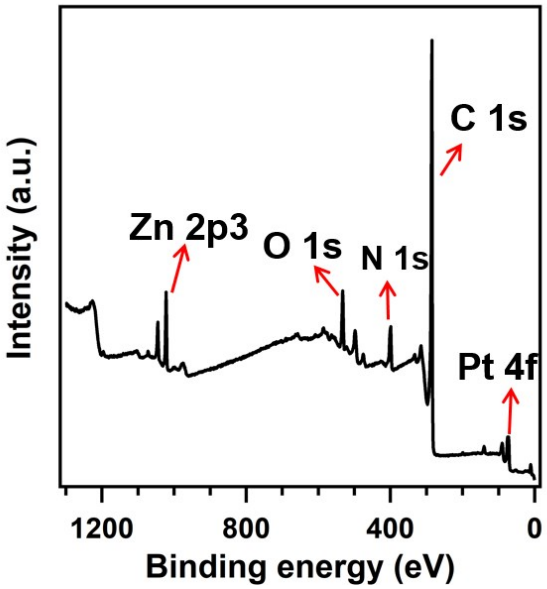

Figure S7. XPS spectra for Pt-COF@MOF_{800}.

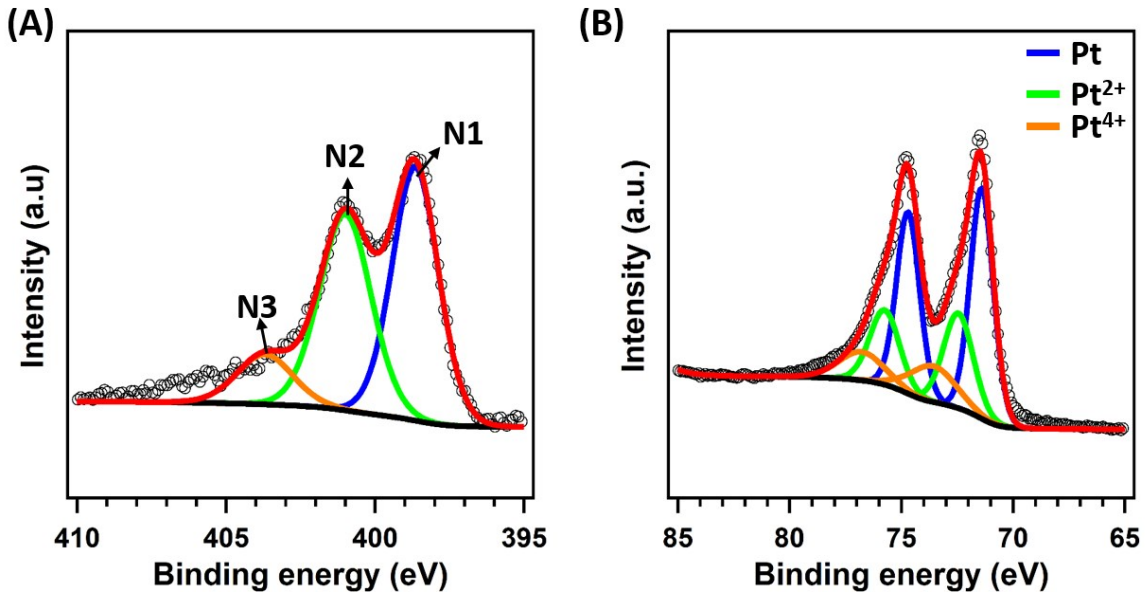

Figure S8. High-resolution XPS spectra of (A) N 1s and (B) Pt 4f for Pt-COF@MOF_{800}.

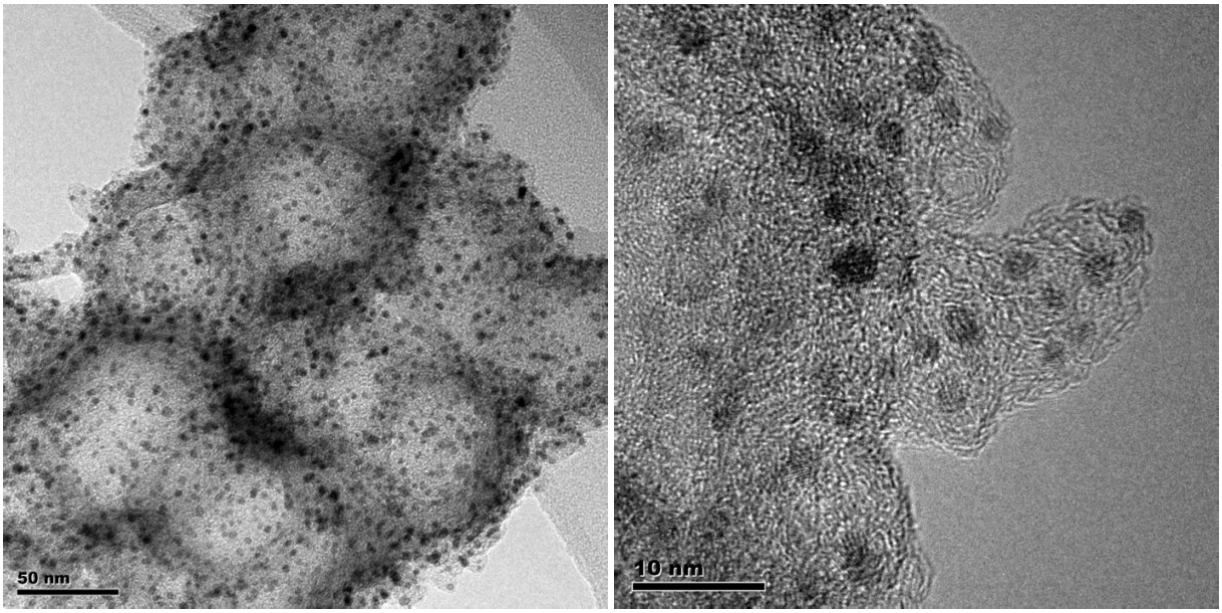

Figure S9. TEM images of Pt-COF@MOF_{800} at different scales.

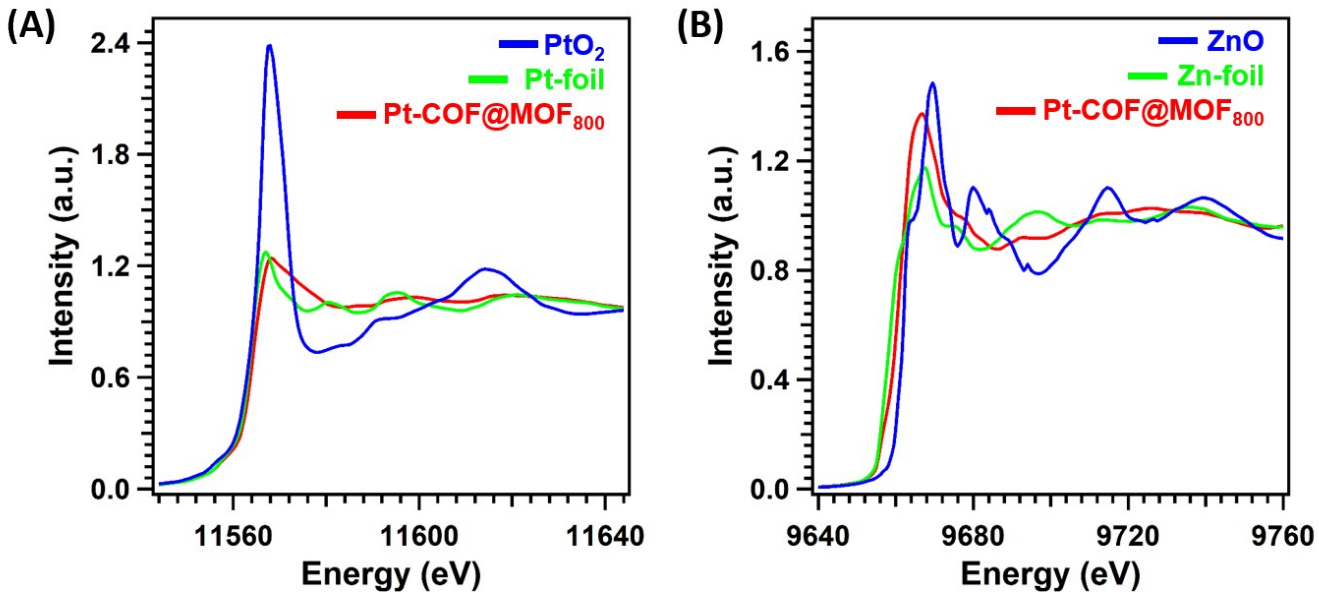

Figure S10. (A) XAFS of Pt-foil (green), PtO_2 (blue) and Pt-COF@MOF (red). (B) XAFS of Zn-foil (green), ZnO (blue) and Pt-COF@MOF (red).

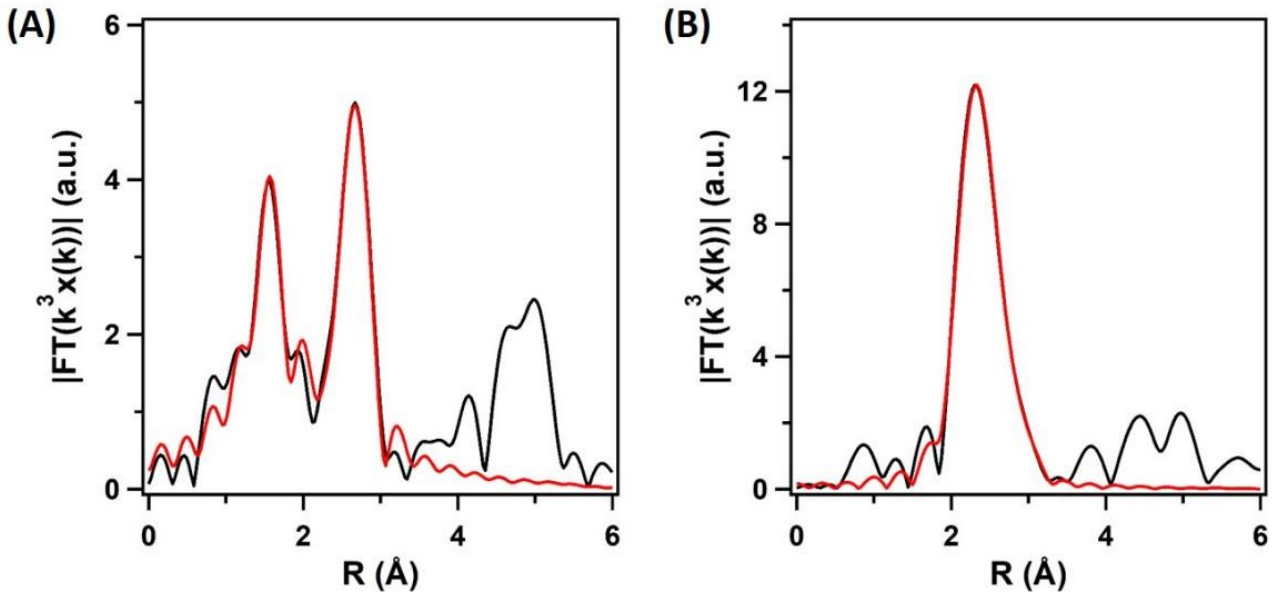

Figure S11. EXAFS fitting curve for (A) Zn and (B) Pt in Pt-COF@MOF_{800}.

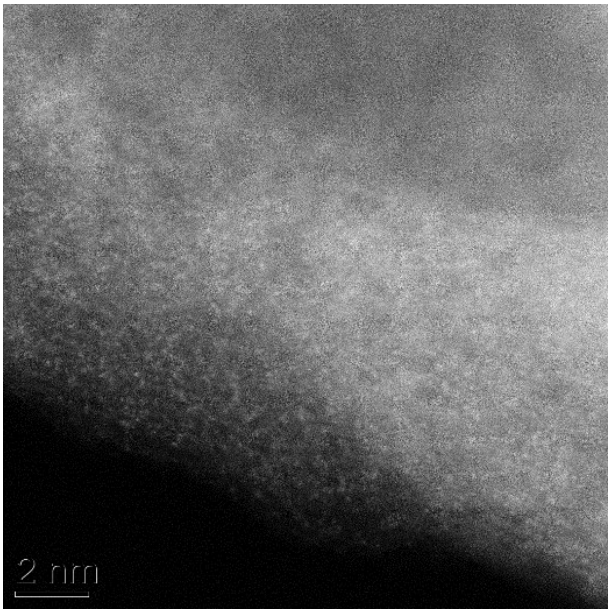

Figure S12. HAADF-STEM images of Pt-COF@MOF_{800}.

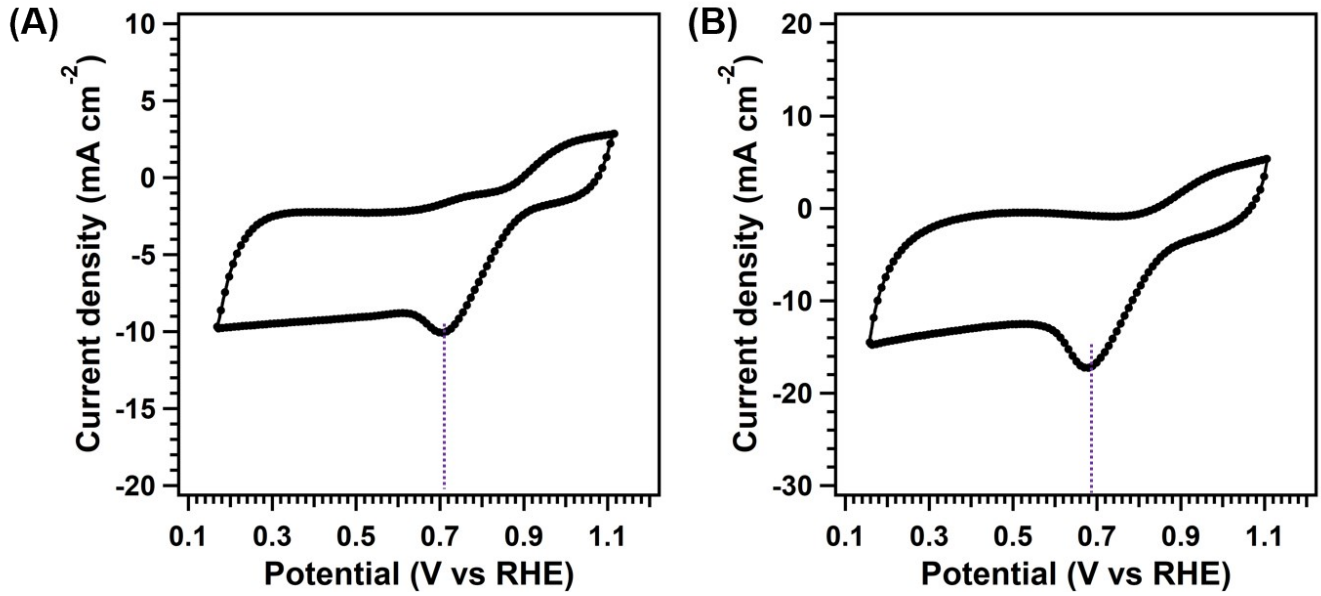

Figure S13. CV curves for Pt-COF@MOF_{800} in 0.1 M KOH (A) and 0.1 M $HClO_4$ (B).

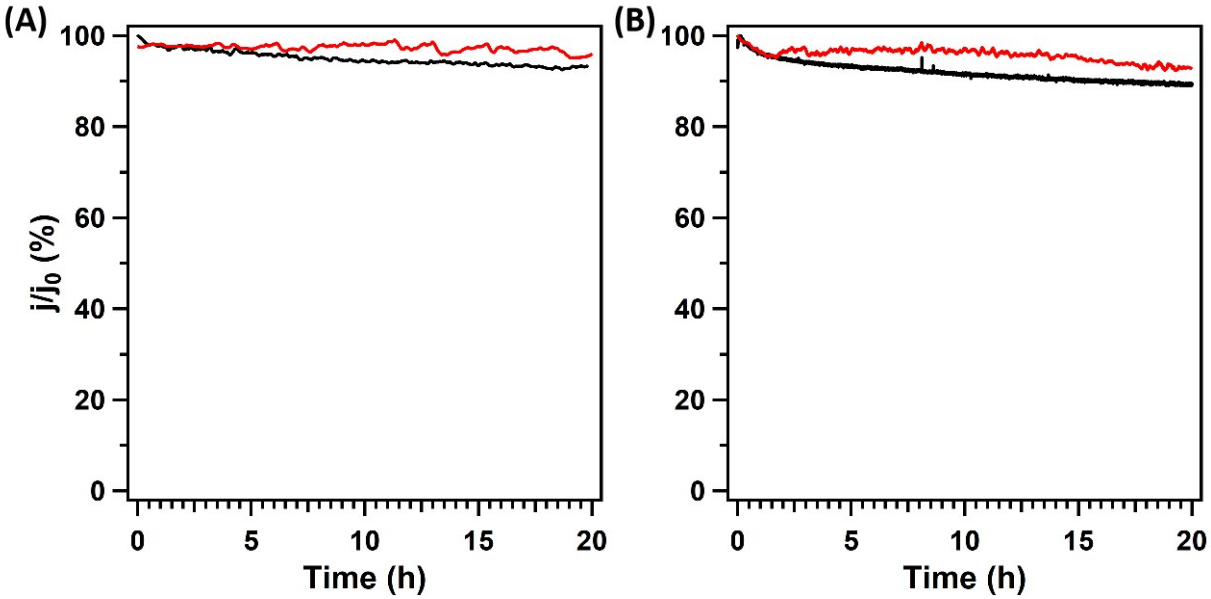

Figure S14. The long-term stability of Pt-COF@MOF_{800} (red curves) and Pt/C (black curves) in alkaline (A) and acidic solution (B) at 0.4 V for 20 hours.

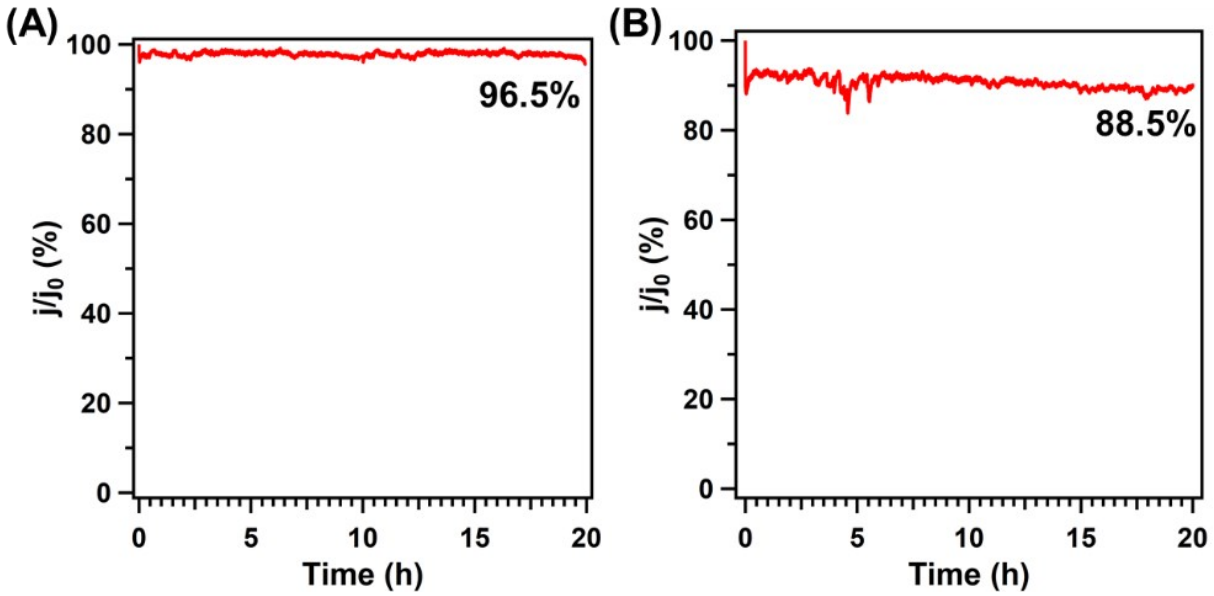

Figure S15. The long-term stability of Pt-COF@MOF_{800} in alkaline (A) and acidic solution (B) at 0.7 V for 20 hours.

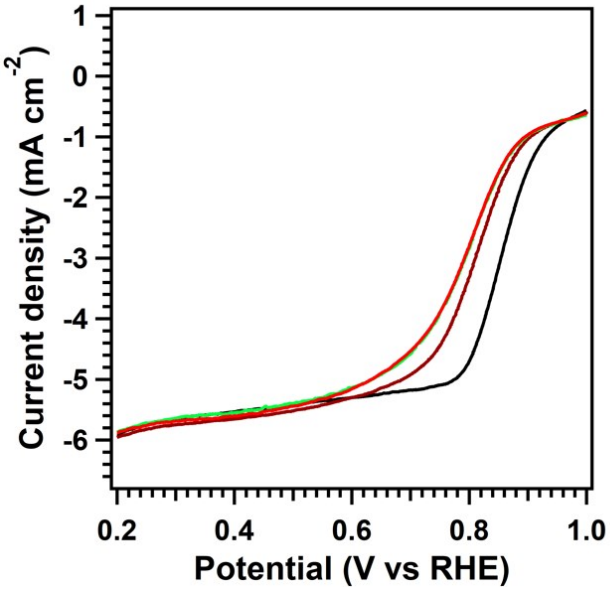

Figure S16. ORR curves of Pt-COF@MOF_{800} before and after different cycles in 0.10 M $HClO_4$. (Black, brown, green and red curves represent initial, after 2000, 4000 and 6000 cycles, respectively.)

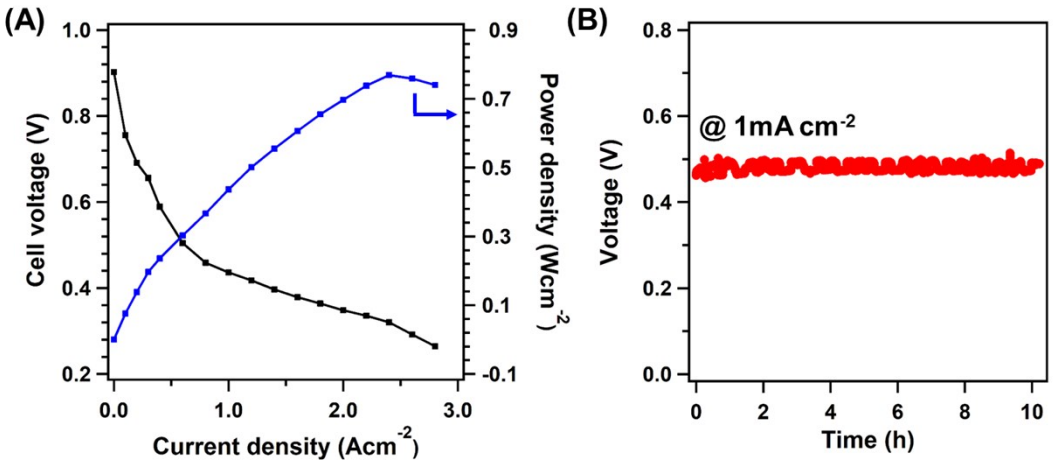

Figure S17. (A) H_2/O_2 fuel cell polarization plots. Cathode: 2 mg cm^{-2} of Pt-COF@MOF_{800}; anode: 0.1 mg cm^{-2} Pt/C; H_2/O_2: 1/0.4 slpm; backpressure: 200 kPa; Temperature: 80 °C. (B) Long-term stability of prepared MEA at a current density of 1 mA cm^{-2} for 10 hours.

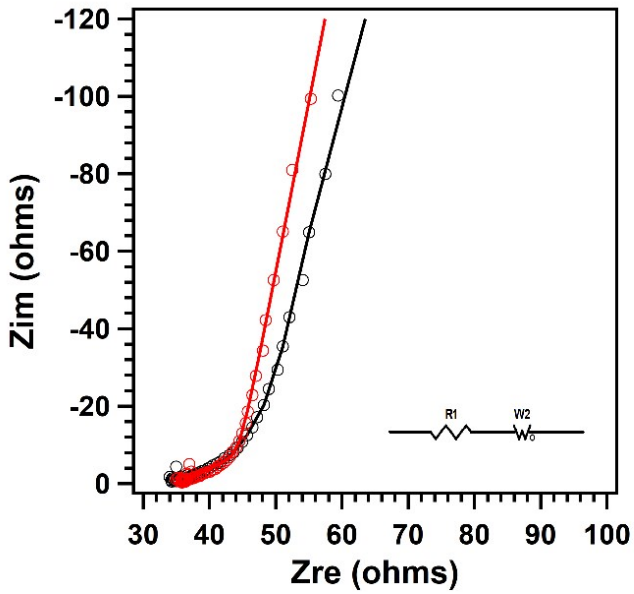

Figure S18. The RIS plots for Pt-COF@MOF_{800} (red curves) and Pt/C (black curves) in 0.1 M KOH solution.

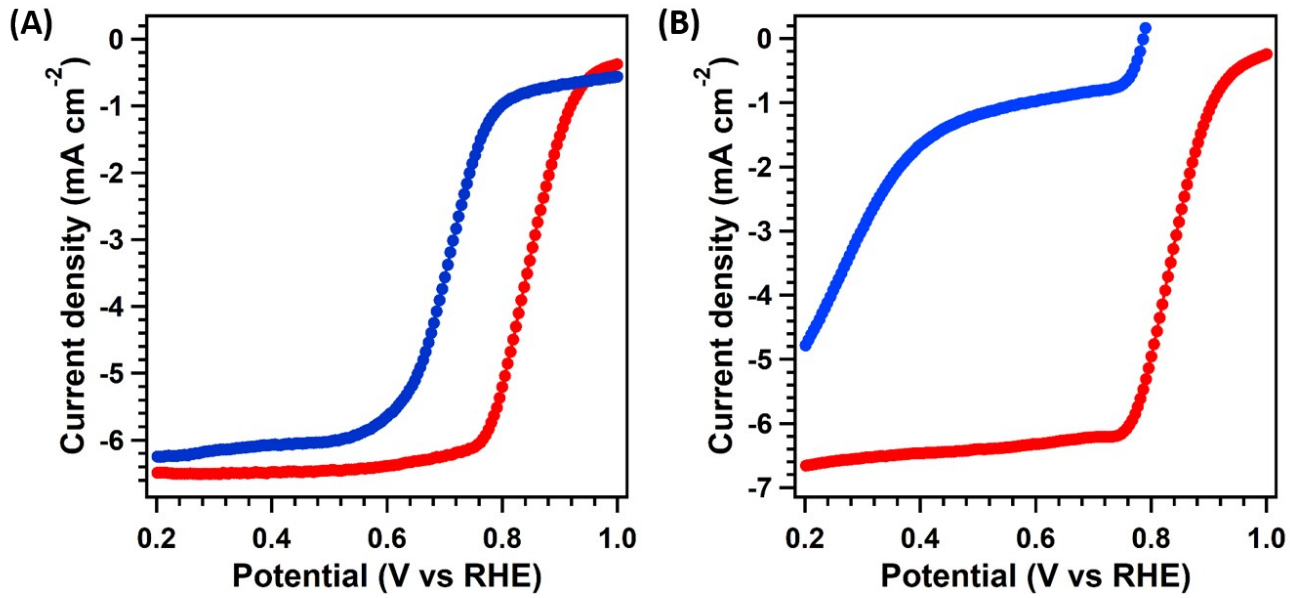

Figure S19. The LSV curves for Pt-COF@MOF_{800} (red curves) and addition of KSCN (blue curves) to the electrolytes in alkaline (A) and acidic (B) condition.

Table S1. K-edge fitting parameters for Pt-COF@MOF_{800}.

Sample	Shell	N	R (Å)	$\sigma^2(10^{-3}Å^2)$	DE_0 (eV)
Pt-COF@MOF_{800}	Zn-N	3.4	2.00	7.5	0.1
	Zn-Pt	3.4	2.65	5.3	13.4
	Zn-Zn	1.9	2.82	4.0	14.0
	Pt-Zn	5.2	2.65	6.4	6.0
	Pt-Pt	7.4	2.79	9.5	5.2

N, coordination number; R, distance between absorber and backscatter atoms; σ^2, Debye-Waller factor to account for both thermal and structural disorders; ΔE_0, inner potential correction; R-factor indicate the goodness of the fit.

Table S2. The kinetic current densities (J_{kin}) for Pt-COF@MOF_{800} and Pt/C at different potentials.

Catalysts	J_{kin} at 0.9 V	J_{kin} at 0.85 V	J_{kin} at 0.8 V
Pt-COF@MOF_{800} (0.1 M $HClO_4$)	1.11	2.71	5.84
Pt/C (0.1 M $HClO_4$)	0.19	1.06	3.88
Pt-COF@MOF_{800} (0.1 M KOH)	1.54	3.50	7.56
Pt/C (0.1 M KOH)	0.91	2.56	7.18

Table S3. The ORR behavior for Pt-COF@MOF_{800} and Pt-based catalysts in acidic condition.

Catalysts	$E_{1/2}$ (V *vs.* RHE)	Eo (V *vs.* RHE)	Tafel slop (mV dec^{-1})	Ref
Pt-COF@MOF_{800}	0.85	1.05	16	This work
Pt/C	0.83	0.97	81	
Pt_1-N/BP	0.76	0.81	/	1
Co@Pd-Pt/CNT	0.85	0.94	/	2
PtP_2 NCs	0.61	0.72	/	3
NPG–Pd–Pt	0.89	0.99	/	4
Pt-Ni@Pt_D/G	0.83	0.99	70	5
Pt-Ni/G	0.78	0.98	156	
40%Pt-$Co_6Mo_6C_2$/^{g}C	0.92	1.06	/	6
$L1_0$-PtCo/C	0.94	0.99	/	7
$Pt_{4.31}$Ga NWs/C	0.75	0.92	131	8
PtTe monolayer	0.90	0.93	/	9
Pd_{20}Au-Pt	0.85	0.99	50	10
37 wt %-FePt/rGO	0.91	0.97	82	11

REFERENCES

1 A. Bhardwaj, J. Kaur, M. Wuest and F. Wuest, *Nat. Commun.*, 2017, **8**, 1.
2 W. Cai, J.-P. Chou, K.-W. Wang, Y.-Y. Hsu, A. Hu, X. Pan and T.-Y. Chen, *Nat. Commun.*, 2019, **10**.
3 H. Li, P. Wen, D. S. Itanze, Z. D. Hood, S. Adhikari, C. Lu, X. Ma, C. C. Dun, L. Jiang, D. L. Carroll, Y. J. Qiu and S. M. Geyer, *Nat. Commun.*, 2020, **11**, 12.
4 J. Li, H.-M. Yin, X.-B. Li, E. Okunishi, Y.-L. Shen, J. He, Z.-K. Tang, W.-X. Wang, E. Yücelen, C. Li, Y. Gong, L. Gu, S. Miao, L.-M. Liu, J. Luo and Y. Ding, *Nat. Energy.*, 2017, 2, 17111.
5 X. Lyu, Y. Jia, X. Mao, D. Li, G. Li, L. Zhuang, X. Wang, D. Yang, Q. Wang, A. Du and X. Yao, *Adv. Mater.*, 2020, **32**, 2003493.
6 X. Ma, H. Meng, M. Cai and P. K. Shen, *J. Am. Chem. Soc.*, 2012, **134**, 1954-1957.
7 J. Liang, N. Li, Z. Zhao, L. Ma, X. Wang, S. Li, X. Liu, T. Wang, Y. Du, G. Lu, J. Han, Y. Huang, D. Su and Q. Li, *Angew. Chem. Int. Ed.*, 2019, **58**, 15471-15477.
8 L. Gao, X. Li, Z. Yao, H. Bai, Y. Lu, C. Ma, S. Lu, Z. Peng, J. Yang, A. Pan and H. Huang, *J. Am. Chem. Soc.*, 2019, **141**, 18083-18090.
9 Y. Wang, Y. Li and T. Heine, *J. Am. Chem. Soc.*, 2018, **140**, 12732-12735.
10 B. Cai, R. Hübner, K. Sasaki, Y. Zhang, D. Su, C. Ziegler, M. B. Vukmirovic, B. Rellinghaus, R. R. Adzic and A. Eychmüller, *Angew. Chem. Int. Ed.*, 2018, **57**, 2963-2966.
11 T. Y. Yoo, J. M. Yoo, A. K. Sinha, M. S. Bootharaju, E. Jung, H. S. Lee, B.-H. Lee, J. Kim, W. H. Antink, Y. M. Kim, J. Lee, E. Lee, D. W. Lee, S.-P. Cho, S. J. Yoo, Y.-E. Sung and T. Hyeon, *J. Am. Chem. Soc.*, 2020, **142**, 14190-14200.